Title

Association of Hepatic Steatosis with Adipose and Muscle Mass and Distribution in Children

Journal

Metabolic Syndrome and Related Disorders, 21(4)

ISSN

1540-4196

Authors

Malki, Ghattas J
Goyal, Nidhi P
Ugalde-Nicalo, Patricia
et al.

Publication Date

2023-05-01

DOI

10.1089/met.2023.0002

Peer reviewed

METABOLIC SYNDROME AND RELATED DISORDERS
Volume 21, Number 4, 2023

Pp. 222–230
DOI: 10.1089/met.2023.0002

Association of Hepatic Steatosis with Adipose and Muscle Mass and Distribution in Children

Ghattas J. Malki, BS,[1] Nidhi P. Goyal, MD, MPH,[1,2] Patricia Ugalde-Nicalo, MD, MAS,[2] Lauren F. Chun, MD,[1] Jasen Zhang, MS,[3] Ziyi Ding, MS,[3] Yingjia Wei, MS,[3] Cynthia Knott, RDN,[4] Danielle Batakis, BS,[5] Walter Henderson, BA,[5] Claude B. Sirlin, MD,[5] Michael S. Middleton, MD, PhD,[5] and Jeffrey B. Schwimmer, MD[1,2]

Abstract

Background: Pediatric studies have shown associations between hepatic steatosis and total body fat, visceral fat, and lean mass. However, these associations have not been assessed simultaneously, leaving their relative importance unknown.
Objective: To evaluate associations between hepatic steatosis and total-body adiposity, visceral adiposity, and lean mass in children.
Method: In children at risk for fatty liver, hepatic steatosis, adipose, and lean mass were estimated with magnetic resonance imaging and dual-energy X-ray absorptiometry.
Results: Two hundred twenty-seven children with mean age 12.1 years had mean percent body fat of 38.9% and mean liver fat of 8.4%. Liver fat was positively associated with total-body adiposity, visceral adiposity, and lean mass ($P < 0.001$), and negatively associated with lean mass percentage ($P < 0.001$). After weight adjustment, liver fat was only positively associated with measures of central adiposity ($P < 0.001$). Visceral adiposity also had the strongest association with liver fat ($P < 0.001$).
Conclusions: In children, hepatic steatosis is more strongly associated with visceral adiposity than total adiposity, and the association of lean mass is not independent of weight or fat mass. These relationships may help guide the choice of future interventions to target hepatic steatosis.

Keywords: hepatic steatosis, MRI-PDFF, adipose, muscle, nonalcoholic fatty liver disease

Introduction

Ectopic lipid accumulation is the buildup of lipids in nonadipose tissue, such as the liver, pancreas, skeletal muscle, bones, and heart. This fat accumulation within organs is a mechanism that can contribute to disease pathogenesis, especially related to metabolic syndrome.[1] In the liver, ectopic lipid accumulation can manifest within hepatocytes as nonalcoholic fatty liver disease (NAFLD), which is defined by hepatic steatosis not due to alcohol consumption or other underlying liver disease,[2] and can progress to cirrhosis, hepatocellular carcinoma, transplantation, and death.[3]

NAFLD currently is the most common chronic liver disease in children, affecting about 10% of the pediatric population in the United States.[4] The incidence of pediatric

[1]Division of Gastroenterology, Hepatology, and Nutrition, Department of Pediatrics, University of California San Diego School of Medicine, La Jolla, California, USA.
[2]Department of Gastroenterology, Rady Children's Hospital, San Diego, California, USA.
[3]Division of Biostatistics and Bioinformatics, University of California San Diego Herbert Wertheim School of Public Health and Human Longevity Science, San Diego, California, USA.
[4]Altman Clinical and Translational Research Institute, School of Medicine, University of California San Diego School of Medicine, La Jolla, California, USA.
[5]Liver Imaging Group, Department of Radiology, University of California San Diego School of Medicine, La Jolla, California, USA.

NAFLD is rising,[5] and it is now the most common cause of liver transplantation in young adults.[6] Pediatric NAFLD is also associated with hepatic and extrahepatic comorbidities, such as type 2 diabetes, hypertension, anxiety, depression, and impaired quality of life.[7–11]

Obesity is a major risk factor for NAFLD in children.[12] However, obesity alone is not sufficient to cause NAFLD in most children. For example, only 25% of children with obesity have NAFLD, and thus the majority do not.[13] Even in adolescents with a median body mass index (BMI) of 52 kg/m^2 undergoing weight loss surgery, 40% had no evidence of steatosis on liver histology.[13,14] Furthermore, although obesity is present in 60% of children with NAFLD, up to 20% have normal BMI percentile, suggesting a nuanced relationship between obesity and NAFLD.[4]

The modest association between BMI and hepatic steatosis has motivated research on the possible relationships between hepatic steatosis and other indices of body composition. For example, greater abdominal visceral fat is associated with metabolic syndrome.[15] Extending this finding to hepatic steatosis, several investigators have reported that abdominal visceral fat correlates more strongly with degree of hepatic steatosis than total-body fat, suggesting that those with higher proportion of abdominal fat stored subcutaneously may be less at risk for developing NAFLD.[12,16,17] Moreover, those with upper-body (*i.e.*, android-type) obesity appear to be more at risk for developing NAFLD than those with lower-body (*i.e.*, gynoid-type) obesity.[18] In adults, degree of hepatic steatosis has been associated with lower skeletal muscle mass,[18,19] suggesting that interplay between muscle and adipose mass may associate with hepatic fat accumulation.[18,20]

Preliminary work in children has shown similar findings, as both lower appendicular and truncal muscle mass have been implicated in pediatric NAFLD.[21,22] However, the association of both adipose and lean mass in pediatric NAFLD have not been assessed together, making it difficult to compare their relative importance.

Uncertainty regarding relationships between hepatic steatosis and indices of body composition is a gap in our understanding of pediatric NAFLD. Thus, the aim of this study was to compare hepatic steatosis with indices of body composition in children, simultaneously considering parameters such as adipose tissue mass, its distribution (android vs. gynoid; visceral vs. subcutaneous), and absolute and relative muscle mass. To accomplish this, we assembled a community-representative cohort of children, measured hepatic steatosis using magnetic resonance imaging proton density fat fraction (MRI-PDFF), and assessed indices of body composition using MRI and dual-energy X-ray absorptiometry (DXA). Gaining insight into relationships between indices of body composition and hepatic steatosis may help our understanding of biological pathways and inform possible therapeutic interventions.

Methods

Participants

We recruited children ages 8–17 years in the County of San Diego from primary care clinics and community health centers. We excluded children with an established diagnosis of chronic liver disease, rheumatologic disease, cerebral palsy, alcohol use, steroid use, neuromuscular diseases, and other conditions affecting lean mass. Patients taking hepatotoxic drugs were also excluded.[23] The study was approved by the Institutional Review Board of the University of California, San Diego (UCSD). The parents of all participants provided written informed consent and HIPAA Authorization. Participants provided written informed assent.

Clinical and laboratory evaluations

Participants were evaluated at the Altman Clinical and Translational Research Institute at UCSD. Participants' age, sex, and self-identified race and ethnicity were recorded, and their height (cm) and weight (kg) were measured. BMI was calculated by dividing the weight (kg) by height squared (m^2). Whole blood was collected to measure fasting serum alanine aminotransferase (ALT), aspartate aminotransferase (AST), gamma-glutamyl transferase (GGT), glucose, and insulin, and to test for viral hepatitis. Study participants completed questionnaires on alcohol use, medications, and past medical history.

Dual-energy X-ray absorptiometry

DXA scans were performed using a fan beam densitometer (Discovery W DXA scanner; Hologic, Marlborough, MA). Data obtained from these scans were used to determine indices of adipose and lean mass measured by Apex software (version 4.0.1; Oracle, Austin, TX). DXA indices reviewed for this study were: subtotal fat mass (kg; total-body adipose mass, excluding that of the skull), subtotal percent fat (%; percent total weight that is body fat, excluding the skull), trunk-to-limb fat mass ratio (kg/kg; truncal adipose mass divided by upper and lower extremity adipose mass), subtotal lean mass (kg; total-body lean mass, excluding that of the skull), appendicular lean mass (kg; lean mass of the upper and lower extremities), subtotal lean mass fraction (kg/kg; subtotal lean mass divided by weight), and appendicular lean mass fraction (kg/kg; appendicular lean mass divided by weight) (Table 1).

The Hologic DXA system integrates the National Center for Health Statistics data of 1200 participants' body compositions, allowing for the generation of *z*-score values for various adiposity and lean mass measures based on sex and age.[24,25] This allowed for the calculation of *z*-score values for BMI, total body percent fat, trunk-to-limb fat mass ratio, and appendicular lean mass/height.[2]

A single technologist performed all scans, as described in the 2019 ISCD Official Positions guidelines.[26] A Hologic spine phantom was used to determine the precision of the collected measurements.[26] The coefficient of variation for phantom DXA measurements was 0.418%.

MRI-PDFF analysis

MRI-PDFF of the liver was estimated using a confounder-corrected chemical-shift-encoded MRI sequence at 3 Tesla (3T), which correlates well with histology-based steatosis grade.[27,28] This method utilizes a 2D gradient-recalled echo acquisition with ≥120 ms repetition time (TR) and low flip angle (10°) to mitigate T1 weighting. Six gradient-recalled echoes were acquired at successive nominal out-of-phase and in-phase echo times (TEs) to permit simultaneous estimation of fractional water and fat signals and T2*

Table 1. Variable Definitions

	Body composition index (U)	*How it was defined*	*How it was measured*
Absolute adipose mass	Subtotal fat mass (kg)	Total-body adipose mass, excluding the skull	DXA
	Subtotal percent fat (%)	Percent total weight that is body fat, excluding the skull	DXA
Body fat distribution	Trunk-to-limb fat mass ratio (kg/kg)	Truncal adipose mass divided by the adipose mass of the upper and lower extremities	DXA
	Percent VAT (%)	The percent of abdominal adipose tissue that is viscerally located	MRI
Absolute lean mass	Subtotal lean mass (kg)	Total-body lean mass, excluding the skull	DXA
	Appendicular lean mass (kg)	Lean mass of the upper and lower extremities	DXA
Relative lean mass	Subtotal lean mass fraction (kg/kg)	Subtotal lean mass divided by weight	DXA
	Appendicular lean mass fraction (kg/kg)	Appendicular lean mass divided by weight	DXA

DXA, dual-energy X-ray absorptiometry; VAT, visceral adipose tissue.

decay.[29–32] A custom algorithm was used to reconstruct MRI-PDFF maps pixel by pixel, correcting for the exponential T2* signal decay and incorporating a multipeak spectral fat model to correct for multifrequency interference effects of fat proton signal.[33]

For each MRI exam, a trained image analyst manually placed one circular region of interest (ROI) with 1-cm radius on an out-of-phase MRI image in all evaluable Couinaud liver segments using Osirix analysis software (Pixmeo SARL, Geneva, Switzerland). ROIs were preferentially placed to avoid liver edges, major blood vessels, major bile ducts, image artifacts, and other organs. ROIs were placed on out-of-phase images rather than quantitative PDFF maps to reduce risk of information bias in their placement. ROIs for each evaluable Couinaud liver segment then were transferred to MRI-PDFF maps without adjustment. Segmental MRI-PDFF values from each of the evaluable ROIs were exported and averaged to calculate a composite MRI-PDFF value for that MRI exam.

Partitioning abdominal adiposity

A 3D gradient dual-echo sequence acquired at 3T was used for subcutaneous adipose tissue (SAT) and visceral adipose tissue (VAT) area segmentation analysis. This 3D dual-echo sequence acquires two echoes per TR: one at a TE value for which fat and water signals are mainly out of phase, and a second at a TE value echo for which fat and water are mainly in phase. Fat and water images were reconstructed automatically by the scanner computer using a two-point Dixon method using the acquired out-of-phase and in-phase data.[34,35]

For each MRI exam, a trained image analyst analyzed fat images using sliceOmatic image segmentation software (TomoVision, Magog, Canada). An axial slice was selected at the level of the umbilicus, and analysis was performed to segment all areas of the image containing SAT and VAT; SAT and VAT were segmented separately. Thresholding tools in the segmentation software and manual tracing by the image analyst were used to avoid regions of the image containing tissues or structures other than SAT or VAT. The total number of pixels contained in the SAT and VAT segmentations were separately exported and converted to surface area units (mm^2). Using these surface areas, the percent VAT, defined as the percent of abdominal fat located viscerally, was calculated as VAT/(VAT+SAT).

Statistical analysis

Anthropometric, demographic, and clinical characteristics of the study population were presented as means (SD) for continuous variables or *N* (%) for categorical variables. Linear regression models were used to calculate the association between MRI-PDFF and various BMIs. The response variable, MRI-PDFF, was logarithmically transformed before analysis to satisfy the normality assumption of linear regression. Multivariate linear regression was first performed to assess associations between each body composition index and liver MRI-PDFF. A series of adjustments were made to control for demographic and biological factors, including the understanding that a higher BMI could be due to more adipose, muscle, or both. In adjustment one of these analyses, demographic covariates such as age, sex, and ethnicity, along with height, were invariably included. In adjustment two, models of adipose and lean indices also included lean or adipose mass as confounders, respectively. Adjustment three accounted for covariates in adjustment one along with weight.

Multivariate linear regression was then performed to determine which body composition indices had the strongest associations with liver MRI-PDFF. Model fitting parameters, including regression estimates (β), correlation coefficients (R^2), and *P* values were used to assess the strength and statistical significance of the associations between BMIs and MRI-PDFF. Because the response variable (MRI-PDFF) was logarithmically transformed, the regression estimates (β) demonstrate how a 1-U change in each of the body indices affects PDFF on a logarithmic scale. Thus, a positive β represents a positive association, while a negative β represents a negative association. A *P* value of <0.05 was considered statistically significant.

Results

Study population

We screened 274 children and excluded 47 as shown in Fig. 1. The remaining 227 children were enrolled in the study and had a mean age of 12.1 ± 2.6 years. Most of our participants were male (61%) and of Hispanic ethnicity (81%). The mean BMI *z*-score was 1.8 ± 0.7, and the mean subtotal percent fat was $38.9\% \pm 8.2\%$. The mean ALT was 32 ± 25 U/L, and the mean liver MRI-PDFF was

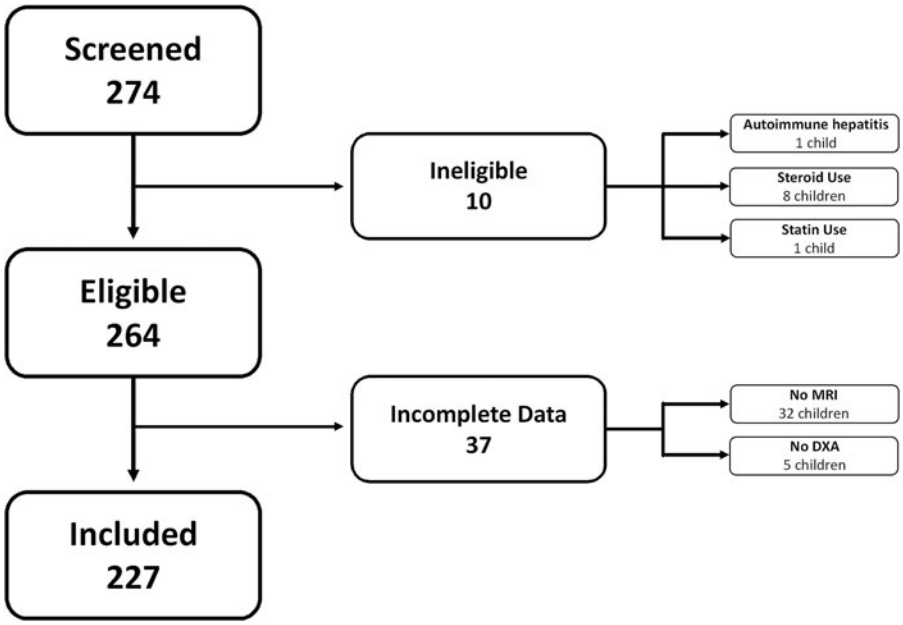

FIG. 1. Study flow diagram showing the recruitment of participants in terms of screening, exclusion, and inclusion. DXA, dual-energy X-ray absorptiometry.

8.4% ± 7.7%. A detailed description of the study participants and their body composition indices are provided (Table 2).

Adipose mass and MRI-PDFF

To assess the association between body fat indices and MRI-PDFF, the following parameters were individually correlated with MRI-PDFF: BMI, BMI *z*-score, subtotal fat mass, and subtotal percent fat. Each parameter was positively associated with MRI-PDFF even after adjusting for age, sex, height, and ethnicity. For example, both BMI and BMI *z*-score showed positive associations with MRI-PDFF ($\beta = 0.590$, $P < 0.001$ and $\beta = 0.575$, $P < 0.001$, respectively) (Table 3, adjustment 1). Additionally, these positive associations between body fat indices and MRI-PDFF were seen in individual multivariate analyses controlling for subtotal lean mass along with age, sex, height, and ethnicity (Table 3, adjustment 2). However, when controlling for weight, total adipose mass indices, including BMI and BMI *z*-score, were no longer associated with MRI-PDFF ($P = 0.195$ and 0.154, respectively) (Table 3, adjustment 3).

Adipose distribution and MRI-PDFF

To assess the association between adipose regionalization and MRI-PDFF, trunk-to-limb fat mass ratio and percent VAT were individually correlated with MRI-PDFF. Similar to total body fat indices, indices of central adiposity were positively associated with MRI-PDFF in multivariable analyses. Trunk-to-limb fat mass ratio and percent VAT were associated with MRI-PDFF even after adjusting for age, sex, ethnicity, and height ($\beta = 2.700$, $P < 0.001$ and $\beta = 2.090$, $P = 0.024$, respectively) (Table 4, adjustment 1). Positive associations between these measures of central adiposity and MRI-PDFF were also seen in individual multivariate analyses controlling for subtotal lean mass, along with age, sex, height, and ethnicity (Table 4, adjustment 2).

Unlike total-body adipose mass, the positive association between centrally localized fat indices and MRI-PDFF remained significant after adjusting for weight, as both the trunk-to-limb fat mass ratio and percent VAT remained positively associated with MRI-PDFF ($\beta = 2.180$, $P < 0.001$ and $\beta = 3.330$, $P < 0.001$, respectively) (Table 4, adjustment 3).

Lean mass and MRI-PDFF

Multivariate linear regression was performed to determine the associations between MRI-PDFF and lean mass, specifically subtotal lean mass, appendicular lean mass, subtotal lean mass fraction, and appendicular lean mass fraction. Notably, when adjusting for age, sex, ethnicity, and height, both subtotal lean mass and appendicular lean mass were positively associated with MRI-PDFF ($\beta = 0.054$, $P < 0.001$ and $\beta = 0.091$, $P < 0.001$, respectively). Accounting for total body weight, both subtotal lean mass fraction and appendicular lean mass fraction were negatively associated with MRI-PDFF ($\beta = -3.650$, $P < 0.001$ and $\beta = -6.810$, $P < 0.001$, respectively) (Table 5, adjustment 1). Once also controlled for subtotal fat mass, subtotal lean mass fraction also became positively associated with MRI-PDFF, while appendicular lean mass fraction was no longer significantly associated (Table 5, adjustment 2). However, all significant associations between lean mass and MRI-PDFF were lost when controlling for weight (Table 5, adjustment 3).

Strength of body composition parameters with MRI-PDFF

Multivariate linear regression was also performed to determine the associations between MRI-PDFF and *z*-score values of body indices, allowing for direct comparison of the strength and significance of absolute adipose mass, body fat localization, and absolute lean mass against each other. The multivariate regression controlling for age, sex, ethnicity, and height again showed that indices for absolute adipose mass, centralized localization of adipose mass, and absolute lean mass were each positively associated with MRI-PDFF. Out of the three domains, adipose distribution had the strongest association, as the trunk-to-limb fat mass ratio *z*-score had the largest effect strength on MRI-PDFF ($\beta = 0.657$, $R^2 = 0.392$, $P < 0.001$) (Table 6).

Table 2. Demographic, Clinical, and Anthropometric Characteristics of the Study Population

Characteristics	*Total (n = 227)*
Age, years (SD)	12.1 (2.6)
Gender, *n* (%)	
Male	138 (0.61)
Female	89 (0.39)
Ethnicity, *n* (%)	
Hispanic or Latino	184 (0.81)
NOT Hispanic or Latino	42 (0.19)
Unknown/not reported	1 (0.0044)
Anthropometric, mean (SD)	
Height, cm	156.2 (13.2)
Weight, kg	69.3 (21.8)
Chemistries, mean (SD)	
ALT, U/L	31.6 (25.2)
AST, U/L	29.1 (12.1)
GGT, U/L	22.2 (11.1)
Glucose, mg/dL	86.4 (9.2)
Insulin, mg/dL	27.3 (27.3)
Liver fat index, % (SD)	
MRI-PDFF	8.4 (7.7)
Absolute adipose indices, mean (SD)	
BMI, kg/m^2	27.8 (5.5)
BMI *z*-score	1.8 (0.7)
Subtotal fat mass, kg	25.3 (10.6)
Subtotal percent fat, %	38.9 (8.2)
Total-body percent fat *z*-score	1.7 (0.7)
Body fat distribution indices, mean (SD)	
Trunk-to-limb fat mass ratio, kg/kg	0.97 (0.19)
Trunk-to-limb fat mass ratio *z*-score	1.4 (0.7)
Percent VAT, %	0.18 (0.07)
Lean mass indices, mean (SD)	
Subtotal lean mass, kg	37.7 (12.6)
Appendicular lean mass, kg	18.1 (6.2)
Appendicular lean mass/height^2 *z*-score	0.6 (1.0)
Subtotal lean mass fraction, %	0.55 (0.07)
Appendicular lean mass fraction, %	0.26 (0.04)

ALT, alanine aminotransferase; AST, aspartate aminotransferase; BMI, body mass index; GGT, gamma-glutamyl transferase; MRI-PDFF, magnetic resonance imaging proton density fat fraction; SD, standard deviation.

A multivariable regression model also suggested that this central regionalization of fat was the strongest predictor of MRI-PDFF. This multivariable regression model compared the strongest predictors from each body composition parameter based on the multivariate analyses in Tables 3–5: subtotal fat mass, trunk-to-limb fat mass ratio, and appendicular lean mass. When controlled for age, sex, ethnicity, and height, both subtotal fat mass and trunk-to-limb fat mass ratio showed positive associations with MRI-PDFF in this regression model ($P < 0.001$), whereas appendicular lean mass was not significantly associated ($P = 0.521$) (Table 7, model 1). When also including weight in this model, only the trunk-to-limb fat mass ratio showed a positive association with MRI-PDFF ($\beta = 2.277$, $P < 0.001$), while the associations between MRI-PDFF with either subtotal fat mass or appendicular lean mass were no longer significant ($P = 0.418$ and 0.799, respectively) (Table 7, model 2).

Discussion

We performed a cross-sectional study in 227 children to assess the relationship between measures of body composition and MRI-PDFF, a biomarker of hepatic steatosis. More specifically, we simultaneously studied body composition domains of total-body adipose, adipose distribution, and total-body lean mass and the relative strength of their associations with hepatic MRI-PDFF. We found that total-body adipose mass, centralized adipose regionalization, and lean mass were all positively associated with higher hepatic MRI-PDFF, whereas subtotal lean mass fraction and appendicular lean mass fraction were negatively associated with hepatic MRI-PDFF. However, after adjusting for weight, only the positive association between centralized adiposity and hepatic MRI-PDFF remained significant. Comparisons of the relative influences of these three indices against each other suggest that centralized fat distribution is more strongly associated with MRI-PDFF than total-body adipose or lean mass.

We first found that indices of adiposity, such as BMI and subtotal fat mass, all positively associated with hepatic MRI-PDFF, suggesting that greater adiposity, independent of where it is stored, is associated with greater hepatic fat. There have been other pediatric studies that have looked at the relationship between measures of total-body adiposity and the severity of hepatic steatosis. Our findings are consistent with two of these studies, in which measures of obesity correlated with measures of steatosis and, more generally, with indices of metabolic syndrome.[12,36] However, the relationship of total adiposity may be more naunced, as

Table 3. Association of Total Adipose with Hepatic Steatosis by Multivariate Analysis

	Individual measures of total adiposity											
	BMI, kg/m^2			*BMI z-score*			*Subtotal fat mass, kg*			*Subtotal percent fat, %*		
	ß	R^2	P	ß	R^2	P	ß	R^2	P	ß	R^2	P
Adjustment 1	**0.590**	**0.296**	<0.001	**0.575**	**0.276**	<0.001	**0.038**	**0.254**	<0.001	**0.040**	**0.217**	<0.001
Adjustment 2	**0.072**	**0.298**	<0.001	**0.465**	**0.284**	<0.001	**0.030**	**0.296**	<0.001	**0.037**	**0.312**	<0.001
Adjustment 3	0.044	0.311	0.195	0.155	0.312	0.154	–0.004	0.305	0.969	0.009	0.312	0.135

Bold means statistically significant ($P < 0.05$).

Adjustment 1: Multivariate analysis controlling for height, age, sex, and ethnicity; Adjustment 2: Multivariate analysis controlling for height, age, sex, ethnicity, and subtotal lean mass; Adjustment 3: Multivariate analysis controlling for height, age, sex, ethnicity, and weight.

The regression estimate (β) demonstrates how a 1-U change in each of the body indices affects PDFF on a logarithmic scale.

Table 4. Association of Adipose Distribution with Hepatic Steatosis by Multivariate Analysis

	Individual measures of adipose distribution					
	Trunk-to-limb fat mass ratio			*Percent VAT*		
	ß	R^2	P	ß	R^2	P
Adjustment 1	**2.700**	**0.406**	<0.001	**2.090**	**0.130**	0.024
Adjustment 2	**2.470**	**0.413**	<0.001	**1.990**	**0.240**	0.022
Adjustment 3	**2.180**	**0.448**	<0.001	**3.330**	**0.348**	<0.001

Bold means statistically significant ($P < 0.05$).

Adjustment 1: Multivariate analysis controlling for height, age, sex, and ethnicity; Adjustment 2: Multivariate analysis controlling for height, age, sex, ethnicity, and subtotal lean mass; Adjustment 3: Multivariate analysis controlling for height, age, sex, ethnicity, and weight.

The regression estimate (β) demonstrates how a 1-U change in each of the body indices affects PDFF on a logarithmic scale.

several pediatric studies have reported no relationship between total body fat and pediatric hepatic steatosis; these studies used either BMI or percent body fat as a measure for adisposity, and were typically conducted in pediatric populations with more severe obesity than our study.[22,37–39] This suggests that the positive relationship between adiposity and hepatic MRI-PDFF is most relevant across the spectrum of BMI percentile, as in our study, but may not be relevant in populations constrained to children with severe obesity.

In addition to total-body adipose, we found that VAT volume is also strongly associated with hepatic MRI-PDFF. The positive relationship between trunk-to-limb fat mass ratio and hepatic MRI-PDFF suggests that fat stored abdominally, rather than in the lower extremities, is associated with increased liver fat. Our findings are consistent with those of Johansen et al., who found that BMI *z*-score and trunk-regional-fat-percent measured by DXA were positively associated with having >1.5% liver fat as measured by MR spectroscopy in Danish children with obesity.[40]

Additionally, we found a positive association between percent VAT with hepatic MRI-PDFF, suggesting that visceral partitioning of fat within the abdomen is correlated with hepatic steatosis. These findings corroborate the conclusions of a 2008 cross-sectional study conducted by Taksali et al. that analyzed the relationship between abdominal fat patterning and hepatic fat fraction in adolescents with obesity. Using MRI to quantify liver fat and VAT, they found that the terciles with a greater proportion of visceral abdominal fat had greater hepatic fat fraction, dyslipidemia, and insulin resistance.[17] In the present study, which included a population with a wider range of BMI, we found that higher visceral fat proportion was associated with higher hepatic MRI-PDFF, even in those participants with milder obesity.

In addition to adiposity, we found that total-body lean mass was positively associated, and that appendicular lean mass fraction was negatively associated with hepatic MRI-PDFF. The positive association between lean mass and MRI-PDFF was surprising, given the protective nature of myokines in preventing systemic inflammation and insulin resistance.[41,42] However, these associations between lean mass and liver MRI-PDFF should be interpreted in the context of the patient's weight and overall total-body fat mass. Because muscle mass is positively associated with BMI,[43] people with higher BMI tend to have more lean mass in general. Thus, BMI is independently positively associated both with hepatic steatosis and with muscle mass, confounding the direct relationship between muscle mass and steatosis. As a result, the positive association of higher lean mass with higher steatosis may be an artifact of the higher BMI of these children.

When controlling for participants' weight, the significant association between lean mass and MRI-PDFF was lost, suggesting that hepatic steatosis is more strongly related to adipose mass. Interestingly, these findings differ from previous work by Yodoshi et al. who found that pediatric NAFLD was negatively associated with both total psoas muscle surface area and total-body muscle mass, even after controlling for age, sex, ethnicity, type 2 diabetes mellitus, and BMI *z*-score. This contradiction may be due to the different severity of disease between the sample populations of these studies. The study population in Yodoshi et al. had a mean BMI *z*-score of ~ 2.4[21] and only included patients diagnosed with NAFLD (mean MRI-PDFF of 22.7%).[22] Because their patients were skewed toward more severe obesity and more severe steatosis, they may have been better able to detect the negative association between muscle mass and liver fat, that we did not find in our study.

However, the higher BMI *z*-scores observed in their study are less representative of many children with NAFLD that have mild-to-moderate obesity. Thus, the findings in our study may be more generalizable, suggesting that muscle mass is commonly not associated with hepatic steatosis accumulation in children.

Through the simultaneous comparison of total adipose mass, adipose distribution, and lean mass, we found that fat distribution had the strongest association with hepatic MRI-PDFF. While greater adipose mass was associated with

Table 5. Association of Total Lean Mass with Hepatic Steatosis by Multivariate Analysis

	Individual measures of total lean mass											
	Subtotal lean mass, kg			*Appendicular lean mass, kg*			*Subtotal lean mass fraction, kg/kg*			*Appendicular lean mass fraction, kg/kg*		
	ß	R^2	P	ß	R^2	P	ß	R^2	P	ß	R^2	P
Adjustment 1	**0.054**	**0.221**	<0.001	**0.091**	**0.190**	<0.001	**−3.650**	**0.180**	<0.001	**−6.810**	**0.180**	<0.001
Adjustment 2	**0.035**	**0.296**	<0.001	**0.059**	**0.286**	0.003	**3.450**	**0.270**	0.033	4.350	0.263	0.114
Adjustment 3	0.006	0.296	0.679	–0.002	0.295	0.946	0.118	0.295	0.908	–0.278	0.296	0.880

Bold means statistically significant ($P < 0.05$).

Adjustment 1: Multivariate analysis controlling for height, age, sex, and ethnicity; Adjustment 2: Multivariate analysis controlling for height, age, sex, ethnicity, and subtotal fat mass; Adjustment 3: Multivariate analysis controlling for height, age, sex, ethnicity, and weight.

The regression estimate (β) demonstrates how a 1-U change in each of the body indices affects PDFF on a logarithmic scale.

Table 6. Association of Body Composition *Z*-Scores with Hepatic Steatosis by Multivariate Analysis

Category	*Measure*	ß	R^2	P
Absolute adipose mass	BMI *z*-score	**0.575**	**0.276**	<0.001
	Total body percent fat *z*-score	**0.466**	**0.210**	<0.001
Body fat distribution	Trunk/limb fat mass ratio *z*-score	**0.657**	**0.392**	<0.001
Absolute lean mass	Appendicular lean mass/height^2 *z*-score	**0.320**	**0.213**	<0.001

Bold means statistically significant ($P < 0.05$).

Multivariate analysis controlling for height, age, sex, and ethnicity. The regression estimate (β) demonstrates how a 1-U change in each of the body indices affects PDFF on a logarithmic scale.

greater liver MRI-PDFF, the regionalization of visceral fat correlated more strongly with hepatic MRI-PDFF. Our results align with a study led by Alferink et al., which evaluated the association of fat and muscle mass with NAFLD in European adults from the Rotterdam Study. Alferink et al. found that centralized adiposity had the strongest association with NAFLD, above both total-body fat and muscle mass.[18] Our study expanded on this finding by extending it to American youth. Interpreted together, these findings suggest that, while BMI may be an uncomplicated way to assess hepatic steatosis risk, it does not account for individual body types and thus does not capture the nuances between body composition and hepatic steatosis. This also suggests that interventions that preferentially decrease VAT may be more likely to decrease hepatic steatosis, although studies are needed to test this hypothesis.

There have been previous studies examining interventions that disproportionately target visceral fat. For example, liraglutide, a GLP-1 receptor agonist, was found to preferentially decrease VAT in adults with overweight or obesity. Along with decreasing liver MRI-PDFF, liraglutide use was associated with a relative reduction in visceral fat that was twice as large as the reduction in overall total-body fat.[44] In addition to pharmacological interventions, a meta-analysis of 39 studies concluded that lower-intensity, high-intensity interval training (HIIT) (80%–90% of peak heart rate) was more successful at reducing abdominal and visceral fat mass, while high-intensity HIIT training (above 90% of maximum heart rate) was more effective at decreasing total-body adiposity.[45] These studies conducted in adults, combined with our data, raise the possibility that pharmacological and exercise interventions exist that could target visceral adipose and, in turn, hepatic steatosis. Studies should test these interventions in children.

Table 7. Multivariable Regression Model Predicting Hepatic Steatosis

	ß	*95% CI*	P
Model 1			
Subtotal fat mass, kg	**0.023**	**0.011 to 0.033**	**<0.001**
Trunk-to-limb fat mass ratio, g/g	**2.275**	**1.716–2.834**	**<0.001**
Appendicular lean mass, kg	0.012	–0.024 to 0.047	0.521
Ethnicity–Hispanic	**0.264**	**0.030 to 0.498**	**0.027**
Gender–Male	**0.250**	**0.052 to 0.449**	**0.014**
Age, years	**−0.113**	**−0.172 to −0.054**	**<0.001**
Height, cm	0.000	–0.017 to 0.017	0.979
Model 2			
Subtotal fat mass, kg	0.024	–0.034 to 0.080	0.418
Trunk-to-limb fat mass ratio, g/g	**2.277**	**1.695 to 2.860**	**<0.001**
Appendicular lean mass, kg	0.013	–0.089 to 0.115	0.799
Ethnicity–Hispanic	**0.265**	**0.027 to 0.503**	**0.030**
Gender–Male	**0.250**	**0.048 to 0.452**	**0.016**
Age, years	**−0.113**	**−0.173 to −0.052**	**<0.001**
Height, cm	0.000	–0.018 to 0.018	0.985
Weight, kg	–0.001	–0.052 to 0.050	0.973

Bold means statistically significant ($P < 0.05$).

Multivariable regression model using a measure of fat mass, fat distribution, and lean mass to predict hepatic steatosis. Model 1 included age, sex, ethnicity, and height; model 2 included age, sex, ethnicity, height, and weight. The regression estimate (β) demonstrates how a 1-U change in each of the body indices affects PDFF on a logarithmic scale.

The strengths of our study include the use of MRI-PDFF and DXA to accurately quantify hepatic steatosis and body composition, respectively. Using these validated techniques allowed for the accurate simultaneous comparison between the strength of fat and lean indices with hepatic steatosis. Additionally, our large, community-based study population allowed us to generalize these findings more broadly. One potential limitation of our study is that the sample population comprised mostly Hispanic children. However, there is a higher prevalence of NAFLD among Hispanic children and, as a result, our study sample reflects a population most at risk. Additionally, we assessed lean mass but did not assess muscle ''quality'' and, thus, did not investigate associations between muscle density or strength with liver fat.

Potential confounders not examined in our study were physical activity and diet composition, which can influence body composition. Visceral and SAT were measured at a single level: the umbilicus; future studies might benefit by total visceral and SAT segmentation. Finally, because of the cross-sectional design of our study, conclusions can only be drawn about correlation, rather than causation.

In conclusion, we found in a population of children at risk for NAFLD that hepatic steatosis was more strongly associated with adipose regionalization than total adipose amount, and the association of lean mass was not independent of fat mass or body weight. Our findings may guide studies to unravel the understanding of biological pathways contributing to hepatic steatosis. Additionally, we speculate that pharmacologic and exercise interventions shown to target visceral fat loss hold promise for decreasing liver fat and propose that such interventions should be evaluated in children for this purpose.

Authors' Contributions

Study concept and design: G.J.M., C.B.S., M.S.M., and J.B.S. Data Generation: N.P.G., P.U.-N., L.F.C., C.K., D.B.,

W.H., C.B.S., M.S.M., and J.B.S. Data analysis: G.J.M., J.Z., Z.D., and Y.W. Data interpretation: G.J.M., N.P.G., J.Z., Z.D. Y.W., M.S.M., and J.B.S. Drafting the article: G.J.M., W.H., and J.B.S. Critical revision of the article: G.J.M., N.P.G., P.U.-N., L.F.C., J.Z., Z.D., Y.W., C.K., D.B., W.H., C.B.S., M.S.M., and J.B.S. Approval of the final article: G.J.M., N.P.G., P.U.-N., L.F.C., J.Z., Z.D., Y.W., C.K., D.B., W.H., C.B.S., M.S.M., and J.B.S.

Disclaimer

The content is solely the responsibility of the authors and does not necessarily represent the official views of the NIH.

Author Disclosure Statement

C.B.S. reports grants to UCSD from American College of Radiology, GE, Siemens, Philips, Bayer, Foundation of NIH, Gilead, and Pfizer; personal consultation fees from Blade, Boehringer, and Epigenomics; consultation under the auspices of the University to AMRA, BMS, Exact Sciences, GE Digital, IBM-Watson, and Pfizer; laboratory service agreements to UCSD from Enanta, Gilead, ICON, Intercept, NuSirt, Shire, Synageva, and Takeda; royalties from Wolters Kluwer for educational material outside the submitted work; honoraria to the UCSD from Medscape for educational material outside the submitted work; pending position as Chief Medical Officer for Livivos; ownership of stock options in Livivos; and unpaid position in advisory board to Quantix Bio.

M.S.M. reports personal consultation fees from Alimentiv, Arrowhead, Glympse, Kowa, Median, and Novo Nordisk; laboratory services agreement through UCSD from Alexion, Astra Zeneca, Bristol-Myers Squibb, Celgene, Enanta, Galmed, Genzyme, Gilead, Intercept, Ionis, Janssen, NuSirt, Organovo, Pfizer, Roche, Sanofi, Shire, Synageva, Takeda, and Quantix Bio; grants to UCSD from Guerbet and Pfizer; personal fees from Livivos and Pfizer, outside the submitted work.

J.B.S. reports grants to UCSD from Intercept, Genfit, and Seraphina, outside the submitted work. All other authors have no conflicts of interest relevant to this article to disclose.

Funding Information

Supported by the National Institutes of Health Grants R56DK090350, UL1TR000100, UL1TR001442, and 1TL1TR001443. The funders did not participate in the conduct of the study; collection, management, analysis, and interpretation of the data; and preparation of the article.

References

1. van Herpen NA, Schrauwen-Hinderling VB. Lipid accumulation in non-adipose tissue and lipotoxicity. Physiol Behav 2008;94(2):231–241.
2. Lindbäck SM, Gabbert C, Johnson BL, et al. Pediatric nonalcoholic fatty liver disease: A comprehensive review. Adv Pediatr 2010;57(1):85–140.
3. Sanyal AJ; American Gastroenterological Association. AGA technical review on nonalcoholic fatty liver disease. Gastroenterology 2002;123(5):1705–1725.
4. Schwimmer JB, Deutsch R, Kahen T, et al. Prevalence of fatty liver in children and adolescents. Pediatrics 2006; 118(4):1388–1393.
5. Sahota AK, Shapiro WL, Newton KP, et al. Incidence of nonalcoholic fatty liver disease in children: 2009–2018. Pediatrics [Internet]. [cited 2021 Sep 5]. 2020;146(6). Available from: https://pediatrics.aappublications.org/content/146/6/e20200771 [Last accessed: September 5, 2021].
6. Wong RJ, Aguilar M, Cheung R, et al. Nonalcoholic steatohepatitis is the second leading etiology of liver disease among adults awaiting liver transplantation in the United States. Gastroenterology 2015;148(3):547–555.
7. Newton KP, Hou J, Crimmins NA, et al. Prevalence of prediabetes and type 2 diabetes in children with nonalcoholic fatty liver disease. JAMA Pediatr 2016;170(10):e161971.
8. Schwimmer JB, Pardee PE, Lavine JE, et al. Cardiovascular risk factors and the metabolic syndrome in pediatric nonalcoholic fatty liver disease. Circulation 2008;118(3): 277–283.
9. Schwimmer JB, Zepeda A, Newton KP, et al. Longitudinal assessment of high blood pressure in children with nonalcoholic fatty liver disease. PLoS One 2014;9(11):e112569.
10. Noon SL, D'Annibale DA, Schwimmer MH, et al. Incidence of depression and anxiety in a cohort of adolescents with nonalcoholic fatty liver disease. J Pediatr Gastroenterol Nutr 2021;72(4):579–583.
11. Kistler KD, Molleston J, Unalp A, et al. Symptoms and quality of life in obese children and adolescents with nonalcoholic fatty liver disease. Aliment Pharmacol Ther 2010;31(3):396–406.
12. Cali AMG, Caprio S. Ectopic fat deposition and the metabolic syndrome in obese children and adolescents. Horm Res Paediatr 2009;71(Suppl. 1):2–7.
13. Yu EL, Golshan S, Harlow KE, et al. Prevalence of nonalcoholic fatty liver disease in children with obesity. J Pediatr 2019;207:64–70.
14. Xanthakos SA, Jenkins TM, Kleiner DE, et al. High prevalence of nonalcoholic fatty liver disease in adolescents undergoing bariatric surgery. Gastroenterology 2015; 149(3):623–634.e8.
15. Goran MI, Gower BA. Relation between visceral fat and disease risk in children and adolescents. Am J Clin Nutr 1999;70(1):149S–156S.
16. Umano GR, Shabanova V, Pierpont B, et al. A low visceral fat proportion, independent of total body fat mass, protects obese adolescent girls against fatty liver and glucose dysregulation: A longitudinal study. Int J Obes 2019;43(4): 673–682.
17. Taksali SE, Caprio S, Dziura J, et al. High visceral and low abdominal subcutaneous fat stores in the obese adolescent: A determinant of an adverse metabolic phenotype. Diabetes 2008;57(2):367–371.
18. Alferink LJM, Trajanoska K, Erler NS, et al. Nonalcoholic fatty liver disease in The Rotterdam Study: About muscle mass, sarcopenia, fat mass, and fat distribution. J Bone Miner Res 2019;34(7):1254–1263.
19. Petta S, Ciminnisi S, Marco VD, et al. Sarcopenia is associated with severe liver fibrosis in patients with nonalcoholic fatty liver disease. Aliment Pharmacol Ther 2017; 45(4):510–518.
20. Miyake T, Miyazaki M, Yoshida O, et al. Relationship between body composition and the histology of nonalcoholic fatty liver disease: a cross-sectional study. BMC Gastroenterol 2021;21:170.
21. Yodoshi T, Orkin S, Romantic E, et al. Impedance-based measures of muscle mass can be used to predict severity of hepatic steatosis in pediatric NAFLD. Nutrition 2021;91–92:111447.

22. Yodoshi T, Orkin S, Arce Clachar AC, et al. Muscle mass is linked to liver disease severity in pediatric nonalcoholic fatty liver disease. J Pediatr 2020;223:93–99.e2.
23. Schwimmer JB, Dunn W, Norman GJ, et al. SAFETY study: Alanine aminotransferase cutoff values are set too high for reliable detection of pediatric chronic liver disease. Gastroenterology 2010;138(4):1357–1364.e2.
24. Kelly TL, Wilson KE, Heymsfield SB. Dual energy X-Ray absorptiometry body composition reference values from NHANES. PLoS One 2009;4(9):e7038.
25. Micklesfield LK, Goedecke JH, Punyanitya M, et al. Dual-energy X-ray performs as well as clinical computed tomography for the measurement of visceral fat. Obes Silver Spring Md 2012;20(5):1109–1114.
26. Shuhart CR, Yeap SS, Anderson PA, et al. Executive Summary of the 2019 ISCD Position Development Conference on Monitoring Treatment, DXA cross-calibration and least significant change, spinal cord injury, periprosthetic and orthopedic bone health, transgender medicine, and pediatrics. J Clin Densitom 2019;22(4):453–471.
27. Schwimmer JB, Middleton MS, Behling C, et al. Magnetic resonance imaging and liver histology as biomarkers of hepatic steatosis in children with nonalcoholic fatty liver disease. Hepatol Baltim Md 2015;61(6):1887–1895.
28. Middleton MS, Van Natta ML, Heba ER, et al. Diagnostic accuracy of magnetic resonance imaging hepatic proton density fat fraction in pediatric nonalcoholic fatty liver disease. Hepatol Baltim Md 2018;67(3):858–872.
29. Bydder M, Yokoo T, Hamilton G, et al. Relaxation effects in the quantification of fat using gradient echo imaging. Magn Reson Imaging 2008;26(3):347–359.
30. Yokoo T, Collins JM, Hanna RF, et al. Effects of intravenous gadolinium administration and flip angle on the assessment of liver fat signal fraction with opposed-phase and in-phase imaging. J Magn Reson Imaging 2008;28(1):246–251.
31. Yokoo T, Bydder M, Hamilton G, et al. Nonalcoholic fatty liver disease: Diagnostic and fat-grading accuracy of low-flip-angle multiecho gradient-recalled-echo MR imaging at 1.5 T. Radiology 2009;251(1):67–76.
32. Yokoo T, Shiehmorteza M, Hamilton G, et al. Estimation of hepatic proton-density fat fraction by using MR imaging at 3.0 T. Radiology 2011;258(3):749–759.
33. Hamilton G, Yokoo T, Bydder M, et al. In vivo characterization of the liver fat ^{1}H MR spectrum. NMR Biomed 2011;24(7):784–790.
34. Ma J. Dixon techniques for water and fat imaging. J Magn Reson Imaging 2008;28(3):543–558.
35. Ma J. Breath-hold water and fat imaging using a dual-echo two-point Dixon technique with an efficient and robust phase-correction algorithm. Magn Reson Med 2004;52(2):415–419.
36. Rehm JL, Wolfgram PM, Hernando D,et al. Proton density fat-fraction is an accurate biomarker of hepatic steatosis in adolescent girls and young women. Eur Radiol 2015;25(10):2921–2930.
37. Deivanayagam S, Mohammed BS, Vitola BE, et al. Nonalcoholic fatty liver disease is associated with hepatic and skeletal muscle insulin resistance in overweight adolescents. Am J Clin Nutr 2008;88(2):257–262.
38. Seth A, Orkin S, Yodoshi T, et al. Severe obesity is associated with liver disease severity in pediatric non-alcoholic fatty liver disease. Pediatr Obes 2020;15(2):e12581.
39. Trout AT, Hunte DE, Mouzaki M, et al. Relationship between abdominal fat stores and liver fat, pancreatic fat, and metabolic comorbidities in a pediatric population with non-alcoholic fatty liver disease. Abdom Radiol 2019;44(9):3107–3114.
40. Johansen MJ, Vonsild Lund MA, Ängquist L, et al. Possible prediction of obesity-related liver disease in children and adolescents using indices of body composition. Pediatr Obes n/a(n/a):e12947.
41. Walsh K. Adipokines, myokines and cardiovascular disease. Circ J 2009;73(1):13–18.
42. Izumiya Y, Hopkins T, Morris C, et al. Fast/Glycolytic muscle fiber growth reduces fat mass and improves metabolic parameters in obese mice. Cell Metab 2008;7(2):159–172.
43. ten Hoor GA, Plasqui G, Schols AMWJ, et al. A benefit of being heavier is being strong: A cross-sectional study in young adults. Sports Med Open 2018;4(1):12.
44. Neeland IJ, Marso SP, Ayers CR, et al. Effects of liraglutide on visceral and ectopic fat in adults with overweight and obesity at high cardiovascular risk: A randomised, double-blind, placebo-controlled, clinical trial. Lancet Diabetes Endocrinol 2021;9(9):595–605.
45. Maillard F, Pereira B, Boisseau N. Effect of high-intensity interval training on total, abdominal and visceral fat mass: A meta-analysis. Sports Med Auckl NZ 2018;48(2):269–288.

Address correspondence to:
Jeffrey B. Schwimmer, MD
Division of Gastroenterology, Hepatology, and Nutrition
Department of Pediatrics
UC San Diego
and Rady Children's Hospital San Diego
3020 Children's Way, MC 5030
San Diego, CA 92123
USA

E-mail: jschwimmer@ucsd.edu